New Microbiologica, 46, 4, 381-389, 2023, ISSN 1121-7138

FULL PAPER

Inhibition of canine parvovirus 2 (CPV-2) replication by TAT-scFv through targeting of the viral structural protein VP2 of CPV-2

Kun Liu[a], Peng Xu[a], Yuchen Li, Jiali Qin, Jiping Zhu, Yi Li

Hubei Engineering Research Center of Viral Vector, Wuhan University of Bioengineering, Hanshi Road, Yangluo Economic Development Zone, Wuhan City, Hubei Province, China

[a]*These authors contributed equally to this work.*

SUMMARY

Canine parvovirus (CPV) causes severe infectious disease with a high mortality rate in dogs. CPV is still a major health issue of dogs in the clinic. Therefore, there is an urgent need to develop effective drugs to treat the disease. In this study, we fused the transactivating transcriptional activator peptide (TAT) with scFv. TAT-scFv was identified by Western blot. CCK8 kit was used to detect the toxicity of TAT-scFv to cells. The binding activity of TAT-scFv to CPV-2-VP2 was detected by DAS ELISA. The cell uptake rate of TAT-scFv was assessed by IFA. After infection with CPV-2, F81 cells were incubated by TAT-scFv. The replication of virus was measured to determine the neutralization effect of TAT-scFv on intracellular and extracellular viruses. Protein docking was used to predict the amino acid (AA) sites of VP2 binding to TAT-scFv. TAT-scFv was expressed in *Escherichia coli* and purified. The DAS ELISA showed that TAT-scFv could bind with CPV-2-VP2. We demonstrated that TAT-scFv entered cells in a dose-dependent and time-dependent manner and effectively inhibited the replication of CPV-2. Using protein docking, we determined the interaction pattern and found that the N-terminal region (AA 41–49) and the C-terminal region (AA 558) of VP2 interacted with the TAT-scFv. Taken together, these results suggest that, TAT-scFv may be a potential antiviral drug for inhibiting CPV-2 replication and controlling disease caused by CPV-2.

Received March 02, 2023 *Accepted* November 09, 2023

INTRODUCTION

Canine parvovirus (CPV) belonging to the genus *Protoparvovirus* within the family *Parvoviridae* causes an acute infectious disease in dogs (Cotmore *et al*., 2019). This disease has a high morbidity rate, strong infectivity and a high mortality rate (Giraldo-Ramirez *et al*., 2020; Jiang HY *et al*., 2021). The viral genome with 5323 nt in length encodes four proteins (VPl, VP2, NSl, NS2). The nonstructural proteins NS1 and NS2 encoded by a 5'-terminal open reading frame (ORF) are early transcriptional regulatory proteins that control viral replication, transcription and assembly. The structural proteins VP1 and VP2 encoded by the 3' ORF are late viral capsid proteins (Perrira CA *et al*., 2007). In addition, the structural protein VP3 can be observed in the mature virion, which is the capsid formed by proteolysis of approximately 19 amino acids (AAs) at the N-terminus of the VP2. The VP2 is the main protective antigen of CPV, accounting for more than 90% of the nucleocapsid proteins of the virus, which shows antigenicity and multiple epitopes (Giraldo-Ramirez *et al*., 2020; Kulkarni MB *et al*., 2019; De la Torre D *et al*., 2018; Li C *et al*., 2019; Callaway HM *et al*., 2017).

A single-chain antibody variable fragment (scFv) connects the heavy chain variable region (VH) of the antibody to the light chain variable region (VL) by elastic short peptide fragments consisting of 10 to 25 Aas (Bird RE *et al*., 1988). ScFv is the smallest functional structural unit with antigen-specific binding activity, with almost identical antigenic affinity to the parent antibody. ScFv has the advantages of strong permeability in cancer cells, low immunogenicity, efficacious expression in prokaryotic systems and simple genetic engineering operations (Power BE *et al*., 2000; Todorova N *et al*., 2021; Smith RA *et al*., 2021; Lim CC *et al*., 2021). ScFv plays an important role in many fields of biology and medicine.

Key words:
Canine parvovirus, VP2, TAT, single-chain antibody variable fragment, replication.

Corresponding author:
Jiping Zhu
E-mail: jp_zhu732@126.com

Green and Frankel first reported that the transactivating transcriptional activator (TAT) of HIV-1 could cross the membrane into the cell and participate in the replication of HIV-1 (Vives E *et al*., 1997). The key factor of the TAT protein determining cell internalization and nuclear transfer is the 47 to 57 basic AA residues (YGRKKRRQRRR), which is called a TAT permeable membrane peptide in the α helix domain (Vives E *et al*., 1997). This short peptide can independently cross multiple types of cell membranes with higher penetration efficiency than that of the full-length TAT protein. TAT exhibits strong biological activity with or without exogenous substances. Some studies showed that TAT carried large exogenous substances into the cell without destroying its biological activity (Lin Y *et al*., 2021; Bei T *et al*., 2021; Lin BY *et al*., 2021).

In this study, the gene sequence of scFv containing the TAT membrane penetrating peptide was synthesized and theTAT-scFv fusion protein was prepared by a prokaryotic expression system. The purified TAT-scFv was found to enter the cell interior and clear intracellular CPV-2 to achieve a rapid cure. Moreover, low cell toxicity of the TAT-scFv has a high potential to become a new way to anti-CPV-2.

MATERIALS AND METHODS

Cells, viruses, and reagents

F81 cells were cultured in Dulbecco's modified Eagle's medium (DMEM, basal media, China) supplemented with 10% fetal bovine serum (FBS) (Nobimpex Biotechnology, Germany). The cells were cultured at 37°C and 5% CO_2. The CPV-2 strain was propagated and titrated in F81 cells and stored at -80°C.

Production of recombinant proteins

TAT-scFv and scFv were synthesized according to the gene sequence of scFv against CPV-2-VP2, which was provided by Professor Yaoming Li (Wuhan University of Bioengineering). There is a linker (GGGGSGGGGS) between TAT (transactivator protein, YGRKKRRQRRR) (Xu Yongting *et al*., 2019) and scFV.

The pET-32a(+) plasmid containing a 6×His tag was used as an expression vector. The corresponding gene fragments were inserted into the pET-32a(+) plasmid digested by *Xho* I and *BamH* I to generate the pTAT-scFv and pscFv, respectively. The plasmids were transformed into *E.coli* BL21 (DE3). The recombinant protein was induced by 1.0 mmol/L IPTG at 37°C for 8 h. The recombinant protein in the inclusion bodies was dissolved in 8 M urea for denaturation and then purified with Ni-NTA His Binding resin (Millipore, USA) under denaturation conditions according to the manufacturer's instructions. The purified protein was dialyzed in renaturation buffer [400 mM L-arginine, 4 mM GSH, 0.4 mM GSSG, 1 M urea, 5% glucose in PBS (pH 7.4)] at 4°C. In subsequent experiments, the refolded protein was dialyzed in 0.01 M PBS, analyzed by SDS-PAGE and Western blots, and stored at -80°C. The VP2 protein, prepared and preserved at -80°C in our laboratory, was obtained by prokaryotic expression (LUO Ru-meng LY *et al*., 2019).

Analysis of cell viability

Cell viability was assessed by Cell Counting Kit-8 (CCK-8) assays (EnoGene, China) with the following modifications. Cells were seeded in 96-well plates with 2×10^4 cells per well and cultured overnight. Then the cells were washed with PBS and incubated with serum-free medium containing different concentrations of TAT-scFv (4, 6, 8, 10 and 12 μM). The cells without TAT-scFv treatment were used as controls. After the cells were cultured for 24 h, cell viability was assessed according to the manufacturer's instructions. The results are expressed as the percentage of optical density of the treated cells relative to the untreated control cells, defined as 100% survival rate.

Cellular uptake of TAT-scFv

F81 cells were seeded in 24-well plates. When cell density reached 70%, the old medium was removed and serum-free medium containing TAT-scFv or scFv was added. After 24 h, the cells were washed with PBS three times, and the TAT-scFv or scFv in the cells was detected by Immunofluorescence assay (IFA).

Inhibition analysis of CPV-2 replication by TAT-scFv

Cells were seeded in 6-well plates and cultured overnight. When cell density reached 70%, the medium was removed, and the cells were infected with CPV-2 for 1 h using an 0.1 $TCID_{50}$. Then, fresh medium containing TAT-scFv or scFv was added to the cells. At 48 h post-infection (hpi), the supernatant, cell lysate, or total cell suspension was collected for virus titration.

Double antibody sandwich ELISA (DAS-ELISA)

DAS-ELISA was used to detect the activity of the refolded TAT-scFv and performed at room temperature. Briefly, a 96-well plate was coated with TAT-scFv or scFv protein at a different concentration (0, 5, 11, 16 μM) and sealed with a sealing solution (2.5% skim milk powder) for 1 h. Then, CPV-2-VP2 (200 ng/well) was added to each well. After 1 hour of reaction, CPV-2-VP2 monoclonal antibody (1:1000) (Shanghai Anyan Trade Co., Ltd., China) was added and incubated for 1 h. HRP-labeled goat anti-rabbit antibody (1:1000) (EnoGene, China) was incubated for 1 h. Tetramethylbenzidine (TMB) was used to develop the color. The OD*450 nm* value of each well was measured by using an automatic ELISA plate reader.

Immunofluorescence assay (IFA)

IFAs were performed with the following modifications. The cells were fixed with 4% paraformaldehyde for 10 minutes and washed with PBS 3 times, and then infiltrated with 0.2% Triton X-100 for 10 minutes. After blocking with 1% BSA for 30 minutes, anti-His antibody (EnoGene, China) was added and incubated for 1 h. Cy3-labeled goat anti-mouse IgG (H+L) (1:500; EnoGene, China) was added to incubate for 1 h, and followed by washing three times. The nuclei were stained with DAPI for 15 minutes. The fluorescence of cell was observed by fluorescence microscopy.

Quantitative real-time PCR

The infected cells were washed with PBS for three times, and viral DNA was extracted for qPCR analysis according to a method described previously (Huang Q *et al*., 2012). The qPCR SYBR was performed with the primers VP2 f (5' TGGTGGTCAACCTGCTGTCAGA 3')/VP2 r (5'TTGATAGCACCCGTAGAAATCCC 3') and the kit of the Green Master Mix with Low ROX (Yeasen, China). Mitochondrial DNA was used as a reference gene, and the primers was f (5' TCAAACTCAAACTACGCCCTG 3')/ r (5' GTTGTGATAAGGGTGGAGAGG 3').

Western blot analysis

Cell protein was isolated by 12% SDS-PAGE and transferred to a polyvinylidene fluoride (PVDF) membrane. The membrane was sealed with 2.5% skim milk at room temperature for 1 h. Then, the membrane was incubated with both mouse anti-His tag monoclonal antibody (1:2000) and anti-β-tubulin antibody (1:3000, ZenBio, China). The membrane was washed three times with PBST and then incubated with HRP-bound goat anti-mouse IgG at a dilution of 1:2000. The reaction was visualized by an ECL chemiluminescence detection system.

Protein docking

The FAST sequences of VP2 and TAT-scFv were identified with the UniProt database. SWISS-MODEL was used for homologous modeling. ZDOCK was used to predict the possible binding sites, and the PyMOL structure with the highest docking score (1670.122) was selected for interaction mode analysis.

Statistical analysis

Student's *t* test and Fisher's exact test were performed using Instat (GraphPad, San Diego, CA). The results were considered significant at a P value of <0.05.

RESULTS

TAT-scFv or scFv showed a binding activity to CPV-2-VP2 in a dose-dependent manner

Although ScFv and TAT-scFv were expressed as inclusion bodies in *E. coli*, the two fusion proteins were highly purified by affinity purification with Ni-NTA resin under denaturing conditions as examined by SDS-PAGE *(Figure 1A*) and Western blot analysis using an anti-His monoclonal antibody (*Figure 1B*). The molecular weights of TAT-scFv and scFv were approximately 25 kDa as indicated by labeled His-tag. To investigate whether the TAT-scFv or scFv is able to bind to the CPV-2-VP2, DAS ELISA was used to detect the antigen reactivity of TAT-scFv or scFv to the CPV-2-VP2. The results showed that TAT-scFv or scFv could effectively bind to CPV-2-VP2 in a dose-dependent manner (*Figure 2*).

TAT-scFv entered F81 cells efficiently

We first assessed the toxicity of TAT-scFv to F81 cells by the CCK-8. The results showed that when the concentration of TAT-scFv was less than 8 μM, the viability of the F81 cells was very close to that of the untreated control cells (*Figure 3*). However, when the concentration of TAT-scFv was equal to or greater than 10 μM, the viability of the F81 cells significantly decreased compared with that of the control cells. The TAT-scFv concentration no more than 8 μM was used for the next experiments.

To investigate the ability of TAT-scFv to enter the cells, TAT-scFv or scFv (8 μM) was added to cells, and

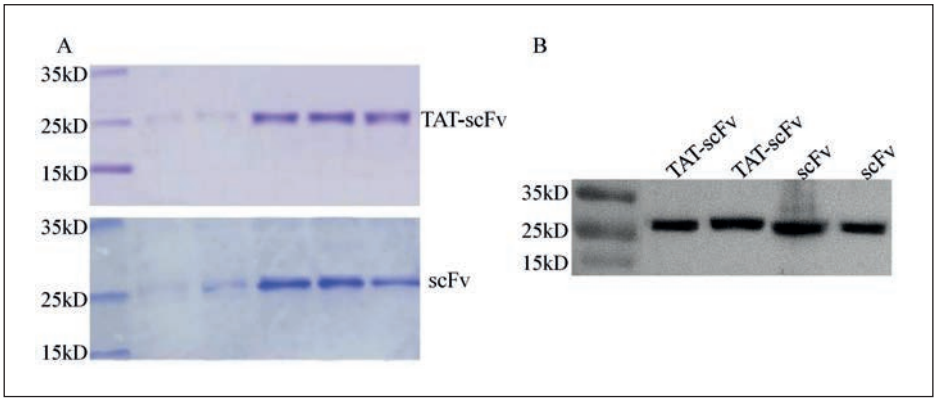

Figure 1 - *Analysis of the purified and refolded TAT-scFv and scFv proteins by SDS-PAGE (A) and Western blots (B).*

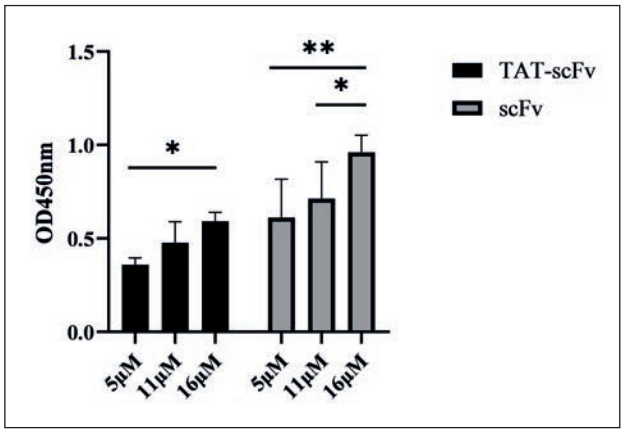

Figure 2 - *Determination of the binding activity of TAT-scFv or scFv to VP2 by DAS ELISAs. Assays were performed in triplicate, and data are presented as the mean ± SD. P values were calculated using ANOVA. *P<0.05; **P<0.01.*

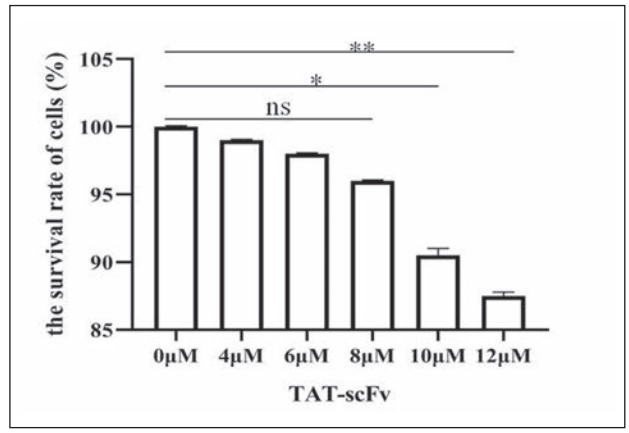

Figure 3 - *Detection of TAT-scFv toxicity using CCK-8 assays. Data are expressed as the mean ± SD of three independent experiments. P values were calculated using ANOVA. *P<0.05 and **P<0.01 compared with the cells incubated with PBS alone (ns = not significant).*

Figure 4 - *Cellular uptake of TAT-scFv or scFv in F81 cells. (A) IFAs. (B) Quantification of intracellular TAT-scFv or scFv.*

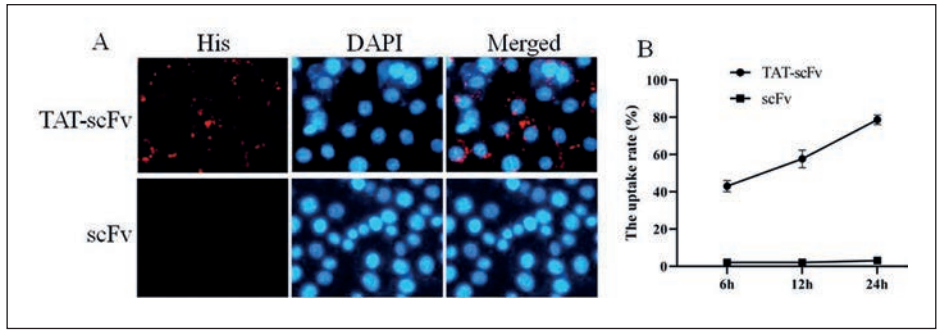

an IFA was performed after 24 h. As shown in *Figure 4A*, TAT-scFv was clearly visible in F81 cells. Conversely, scFv without TAT was almost undetectable in cells. Cell images were divided into groups of 10, and the cells in the three groups were counted to calculate the uptake rate of TAT-scFv or scFv. The results indicated that the distribution of TAT-scFv reached approximately 80% in the cells after 24 h compared to the scFv (*Figure 4B*).

TAT-scFv inhibited significantly CPV-2 replication in F81 cells

To determine whether TAT-scFv can specifically bind to CPV, F81 cells were co-incubated with TAT-scFv and CPV. After 36 h, indirect immunofluorescence technology was used to analyze the subcellular localization of TAT-scFv and CPV. The results showed that there was co-localization between TAT-scFv and CPV, indicating that TAT-scFv can specifically bind to CPV (*Figure 5A*).

To evaluate the ability of TAT-scFv and scFv to inhibit CPV-2 infection, different concentrations of TAT-scFv or scFv were added to the infected cells as described in the materials and methods. The cytopathic effects (CPEs) were observed after 48 h. The results showed that as the TAT-scFv concentration increased the cytopathic effect gradually decreased and the boundary of the F81 cells became clearer (*Figure 5B*). No obvious CPEs were observed when the concentration of TAT-scFv reached 4 μM. The inhibitory effect of scFv on the CPEs of the infected cells was weaker than that of TAT-scFv, suggesting that both TAT-scFv and scFv inhibit CPV-2 infection in a dose-dependent manner.

We next tested the contents of progeny virus from the cell culture supernatant, cell lysate and total cell suspension by $TCID_{50}$ analysis to further confirm the inhibitory activity of TAT-scFv and scFv on the viral replication. Our results once again demonstrated that the TAT-scFv was more effective in inhibiting CPV-2 than scFv (*Figure 6A*) and that CPV-2 replication was dramatically inhibited both intracellularly and extracellularly after culture with 4 μM TAT-scFv at 48 hpi (*Figure 6B, 6C*). However, scFv effectively inhibited only the extracellular CPV-2, indicating that the TAT-scFv showed a more effective inhibitory ef-

fect on the virus replication compared with the scFv. To further determine the effect of TAT-scFv to inhibit CPV-2 replication, we used qPCR to detect the *vp2* DNA. The data showed that the *vp2* gene was significantly inhibited as the concentration of TAT-scFv increased, the relative replication level of *vp2* gene was significantly decreased after cells were cultured with 4 μM TAT-scFv at 24 hpi in a time-dependent manner (*Figure 7A*), and the *vp2* gene replication was decreased with 2 μM TAT-scFv treatment but not for scFv (*Figura 7B*). These results revealed that TAT-scFv had a better inhibitory effect on viral DNA replication than scFv.

The N-terminal of VP2 was the main region of interaction with the TAT-scFv

ZDOCK was used to predict possible binding sites, and the PyMOL structure with the highest docking score (1670.122) was selected for interaction mode analysis. The interaction mode (*Figure 8*) diagram

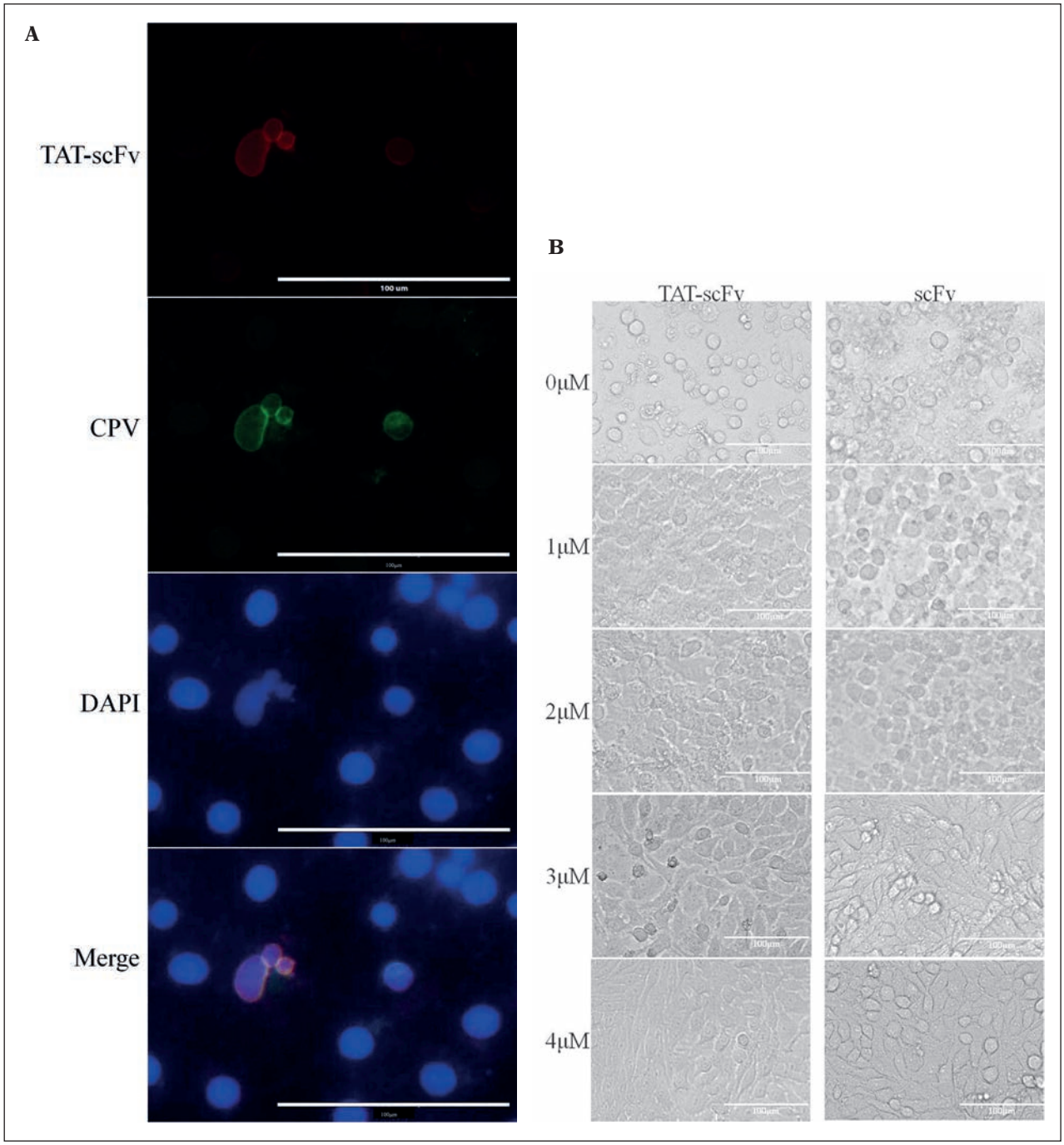

Figure 5 - *Co-localization of TAT-scFv and CPV (A), and Morphological observation (CPEs) of the CPV-2-infected cells after incubation with TAT-scFv or scFv (B).*

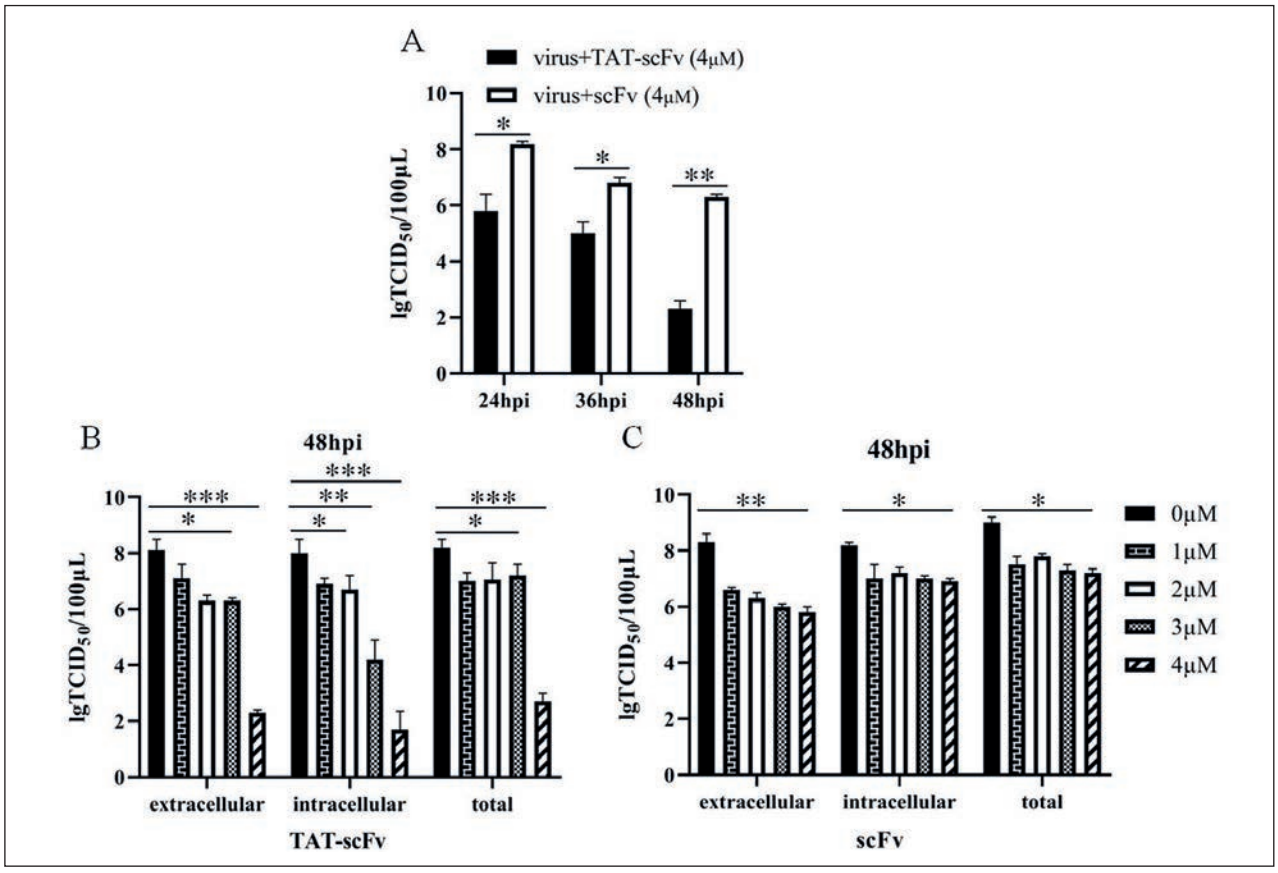

Figure 6 - *Inhibition of CPV-2 replication by TAT-scFv or scFv in F81 cells. F81 cells were infected with CPV-2 for 1 h, and then, the cell culture media were replaced with fresh DMEM containing TAT-scFv or scFv at the indicated concentrations. (A) Progeny viruses were measured at 24 hpi, 36 hpi and 48 hpi by $TCID_{50}$. (B) Intracellular progeny virus, extracellular virus or total progeny virus was measured at 48 hpi by $TCID_{50}$. Data are expressed as the mean ± SD of three independent experiments. P values were calculated using ANOVA. *P<0.05, **P<0.01 and ***P<0.001.*

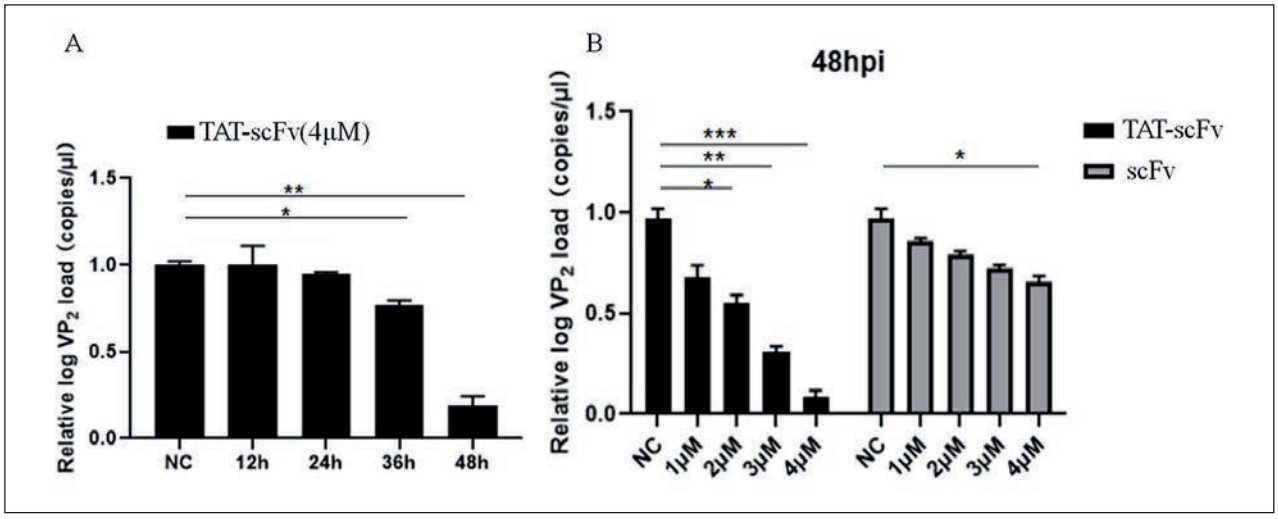

Figure 7 - *Relative levels of CPV-2 DNA were detected by qPCR using VP2-specific primers. (A) CPV-2-infected cells treated with TAT-scFv. Relative levels of CPV-2 DNA were detected at different time points. (B) CPV-2-infected cells were incubated with TAT-scFv or scFv at the indicated concentrations. Relative levels of CPV-2 DNA were detected at 48 hpi. Mitochondrial DNA levels served as an internal reference. Data are expressed as the mean ± SD of three independent experiments. P values were calculated using ANOVA. *P<0.05, **P<0.01 and ***P<0.001.*

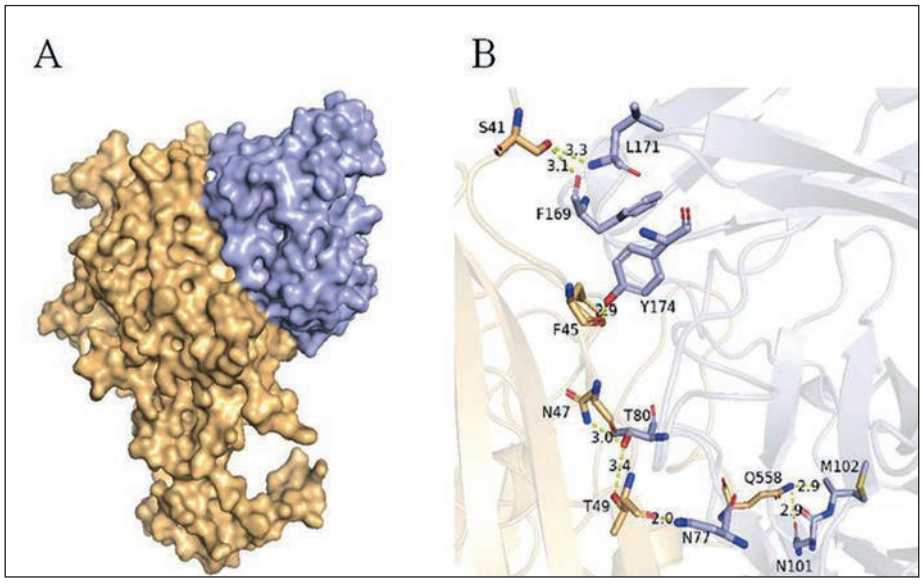

Figure 8 - *Prediction of docking between TAT-V and VP2. (A) A three-dimensional diagram of the TAT-scFv and VP2 interaction. Blue indicates TAT-V, and yellow indicates VP2. (B) Interacting residues of TAT-V and VP2 in a zoomed-in view of the ribbon diagram.*

shows that S41 of VP2 forms two hydrogen bonds with L171 and F169 of TAT-scFv, and the length of hydrogen bonds is 3.3 Å and 3.1 Å, respectively. F45 of VP2 and Y174 of TAT-scFv form a hydrogen bond with a length of 2.9 Å. N47 and T49 of VP2 and T80 of TAT-scFv form hydrogen bonds with a length of 3.0 Å and 3.4 Å, respectively. T49 of VP2 forms a hydrogen bond with N77 of TAT-scFv, and the length of the hydrogen bond is 2.0 Å. Q558 of VP2 forms a hydrogen bond with N101 and M102 of TAT-scFv, and the length of hydrogen bonds is 2.9 Å and 2.9 Å, respectively. The above residues may be the main AAs for their interactions.

DISCUSSION

Diseases caused by CPV-2 are common canine illnesses. Although dogs have been widely vaccinated, there are frequent reports of failed immunizations. Some studies have reported that the *vp2* gene is constantly mutating, resulting in antigenic changes in CPV-2, which poses a challenge to the effectiveness of CPV-2 vaccines (Battilani M et al., 2019; Ahmed N *et al.*, 2018).

Genetically engineered antibodies are generally considered superior to conventional ones in terms of treatment. Cell transmembrane peptides are often coupled with nanoantibodies because they can carry exogenous substances into cells and improve therapeutic efficiency (Wender PA *et al.*, 2002). Among them, the most widely studied cell-penetrating peptide is TAT, which is nontoxic to host cells within a certain concentration range and can bring foreign substances into the cell without affecting its biological characteristics. In the study of topical ocular administration, the cellular internalization of the simulated drug TAT-lip occurs through electrostatic interactions with the cell membrane and shows energy dependence (Wu B *et al.*, 2021).

In this study, the prokaryotic expression plasmids pTAT-scFv and pscFv were constructed to express the fusion proteins with a His tag at the C-terminus. To maintain the activity of TAT and scFv, we linked the C-terminus of TAT to scFv by a linker. Flexible linkers are often used to connect functional domains in fusion proteins. This linker has a simple structure, good flexibility and solubility, and has little effect on the structure and activity of fusion proteins (Chen K *et al.*, 2013; Ghadaksaz A *et al.*, 2021).

Both TAT-scFv and scFv could effectively bind VP2 detected by DAS ELISA, but the binding efficiency of scFv with VP2 was higher than that of TAT-scFv. This may be due to the influence of external TAT insertion on the structure of scFv, which reduced the binding efficiency. However, the activity of TAT-scFv in cells was not affected and the distribution of TAT-scFv reached approximately 80% after 24 h, while only a small amount of scFv entered the cells, indicating that the TAT-scFV penetrated F81 cells efficiently.

Membrane-penetrating peptides are widely used because they can bind various biomolecules through covalent bonds or physical complexation. The most valuable role of these peptides is as a delivery vehicle to promote the efficacy of drugs in the treatment of diseases. The ability to deliver drugs and other therapeutic molecules into cells indicates the therapeutic potential of transmembrane peptides (Xie Y *et al.*, 2019). TAT peptides can be combined with other antiviral drugs to enter cells and even cross the blood-brain barrier to neutralize viruses, including hepatitis B virus and rabies virus (Nakajima O *et al.*, 2003; Phoolcharoen W *et al.*, 2017; Zhang JF *et al.*, 2018).

Both TAT-scFv and scFv could inhibit the production of CPV-2 progeny with the extension of incubation time. TAT-scFv was more effective in suppressing the virus than scFv. With increasing TAT-scFv concentration, both intracellular and extracellular viruses were significantly inhibited. When scFv was co-incubated with CPV-2-infected cells, the progeny virus replication was also inhibited to a certain extent, but the extracellular virus was mainly inhibited, and the inhibitory effect on the intracellular virus titer was poor. Our results demonstrated that a novel antibody conjugated with a TAT molecule against CPV-2-VP2 effectively inhibited the extracellular and intracellular virus replication.

Protein docking analysis showed that TAT-scFv mainly binds to residues S41, F45, N47, T49, and Q558 of VP2. The VP2 of the CPV-2 is the main component of the capsid protein, which plays an important role in inducing specific antibodies and determins host range. Previous reports have shown that mutations in key AAs in VP2 lead to changes in the antigenic properties and host range of CPV-2. These changes determine the antigenic drift and evolution of CPV-2 (Jiang HY *et al*., 2021; Gainor K *et al*., 2021; Hao X *et al*., 2020). The epidemiological investigation of CPV-2 showed that residues S41, F45, N47, T49, and Q558 of VP2 were not high-frequency mutation sites (Rongguang Lu YY *et al*., 2020; Allison AB *et al*., 2016; Tsao J *et al*., 1991), suggesting that TAT-scFv might have a broad-spectrum anti-CPV-2 effect.

In summary, in this study, we prepared a highly efficient membrane penetrating protein, TAT-scFv. This recombinant protein neutralized both intracellular and extracellular CPV-2 and significantly inhibited CPV-2 infection. Predictive analysis shows that TAT-scFv interacts mainly with S418, F45, N47, T49, and Q558 of CPV-2-VP2. These AA sites are conserved in most CPV-2 viruses, suggesting that TAT-scFv may have a specific anti-CPV-2 effect. This study provides ideas and an experimental basis for the development of new anti-CPV-2 drugs.

Acknowledgements

This work was supported by the National Natural Science Foundation of China (grant numbers 31470268) and Natural Science Foundation of Hubei Province (grant numbers 2019CFB310). We thank Lilan Xie and Xiaoming Li for assistance with the experimental technology.

Ethical Approval statement

The viruses in this study are kept in our laboratory and do not involve materials requiring ethical approval. Ethical approval was not therefore required for this study.

Conflict of interests

The authors declare no conflict of interests.

References

Ahmed N., Riaz A., Zubair Z., Saqib M., Ijaz S., Nawaz-Ul-Rehman MS., et al. (2018). Molecular analysis of partial VP-2 gene amplified from rectal swab samples of diarrheic dogs in Pakistan confirms the circulation of canine parvovirus genetic variant CPV-2a and detects sequences of feline panleukopenia virus (FPV). *Virology journal*. **15** (1), 45.

Allison A.B., Organtini L.J., Zhang S., Hafenstein S.L, Holmes E.C., Parrish C.R. (2016). Single Mutations in the VP2 300 Loop Region of the Three-Fold Spike of the Carnivore Parvovirus Capsid Can Determine Host Range. *Journal of virology*. **90** (2), 753-767.

Battilani M., Modugno F., Mira F., Purpari G., Di Bella S., Guercio A,. Balboni A. (2019). Molecular epidemiology of canine parvovirus type 2 in Italy from 1994 to 2017: recurrence of the CPV-2b variant. *BMC veterinary research*. **15** (1), 393.

Bei T., Cao X., Liu Y., Li J., Luo H., Huang L., et al. (2021). Antioxidant Fusion Protein SOD1-Tat Increases the Engraftment Efficiency of Total Bone Marrow Cells in Irradiated Mice. *Molecules*. **26** (11), 3395.

Bird R.E., Hardman K.D., Jacobson J.W., Johnson S., Kaufman B.M., Lee S.M, et al. (1988). Single-chain antigen-binding proteins. *Science*. **242** (4877), 423-426.

Callaway H.M., Feng K.H., Lee D.W., Allison A.B., Pinard M., McKenna R., et al. (2017). Parvovirus Capsid Structures Required for Infection: Mutations Controlling Receptor Recognition and Protease Cleavages. *Journal of virology*. **91** (2), e01871-16.

Chen K., Liu S., Wang G., Zhang D., Du G., Chen J., Shi Z. (2013). Enhancement of Streptomyces transglutaminase activity and pro-peptide cleavage efficiency by introducing linker peptide in the C-terminus of the pro-peptide. *Journal of industrial microbiology & biotechnology*. **40** (3-4), 317-325.

Cotmore S.F., Agbandje-McKenna M., Canuti M., Chiorini J.A., Eis-Hubinger A.M., Hughes J., et al. (2019). ICTV Virus Taxonomy Profile: Parvoviridae. *The Journal of general virology*. **100** (3), 367-368.

De la Torre D., Mafla E., Puga B., Erazo L., Astolfi-Ferreira C., Ferreira A.P. (2018). Molecular characterization of canine parvovirus variants (CPV-2a, CPV-2b, and CPV-2c) based on the VP2 gene in affected domestic dogs in Ecuador. *Veterinary world*. **11** (4), 480-487.

Gainor K., Bowen A., Bolfa P., Peda A., Malik Y.S., Ghosh S. (2021). Molecular Investigation of Canine Parvovirus-2 (CPV-2) Outbreak in Nevis Island: Analysis of the Nearly Complete Genomes of CPV-2 Strains from the Caribbean Region. *Viruses*. **13** (6), 1083.

Ghadaksaz A., Imani Fooladi A.A., Mahmoodzadeh Hosseini H., Nejad Satari T., Amin M. (2021). ARA-linker-TGFalphaL3: a novel chimera protein to target breast cancer cells. *Med Oncol*. **38** (8), 96.

Giraldo-Ramirez S., Rendon-Marin S., Ruiz-Saenz J. (2020). Phylogenetic, Evolutionary and Structural Analysis of Canine Parvovirus (CPV-2) Antigenic Variants Circulating in Colombia. *Viruses*. **12** (5), 500.

Hao X., He Y., Wang C., Xiao W., Liu R., Xiao .X, Zhou .P, Li S. (2020). The increasing prevalence of CPV-2c in domestic dogs in China. *PeerJ*. **8**, e9869.

Huang Q., Deng X., Yan Z., Cheng F., Luo Y., Shen W., et al. (2012). Establishment of a reverse genetics system for studying human bocavirus in human airway epithelia. *PLoS pathogens*. **8** (8), e1002899.

Jiang H., Yu Y., Yang R., Zhang S., Wang D., Jiang Y., et al. (2021). Detection and molecular epidemiology of canine parvovirus type 2 (CPV-2) circulating in Jilin Province, Northeast China. *Comparative immunology, microbiology and infectious diseases*. **74**, 101602.

Kulkarni M.B., Deshpande A.R., Gaikwad S.S., Majee S.B., Suryawanshi P.R., Awandkar S.P. (2019). Molecular epidemiology of Canine parvovirus shows CPV-2a genotype circulating in dogs from western India. *Infection, genetics and evolution: journal of molecular epidemiology and evolutionary genetics in infectious diseases*. **75**, 103987.

Li C., Tang J., Chen Z., Niu G., Liu G. (2019). A divergent canine parvovirus type 2c (CPV-2c) isolate circulating in China. *Infection, genetics and evolution: journal of molecular epidemiology and evolutionary genetics in infectious diseases*. **73**, 242-247.

Lim C.C., Chan S.K., Lim Y.Y., Ishikawa Y., Choong Y.S., Nagaoka Y., Lim T.S. (2021). Development and structural characterisation of human scFv targeting MDM2 spliced variant MDM2(15kDa). *Molecular immunology*. **135**, 191-203.

Lin B.Y., Zheng G.T., Teng K.W., Chang J.Y., Lee C.C., Liao P.C., Kao M.C. (2021). TAT-Conjugated NDUFS8 Can Be Transduced into Mitochondria in a Membrane-Potential-Independent Manner and Rescue Complex I Deficiency. *International journal of molecular sciences*. **22** (12), 6524.

Lin Y., Wan Y., Du X., Li J., Wei J., Li T., et al. (2021). TAT-modified serum albumin nanoparticles for sustained-release of tetramethylpyrazine and improved targeting to spinal cord injury. *Journal of nanobiotechnology*. **19** (1), 28.

LUO Ru-meng L.Y., ZHU Ji-ping, LI Yi. (2019). Establishment of HEK293T cell lines stably expressing canine parvovirus structural protein VP2 by CRISPR/Cas9. *Chin J Vet Sci*. **39** (8): 1476-1483.

Nakajima O., Hachisuka A., Teshima R., Sawada J. (2003). Study on a method for delivering scFv recombinant antibody into cultured cells. *Bulletin of National Institute of Health Sciences*. **121**, 34-39.

Pereira C.A., Leal E.S., Durigon E.L. (2007). Selective regimen shift and demographic growth increase associated with the emergence of high-fitness variants of canine parvovirus. *Infection, genetics and evolution: journal of molecular epidemiology and evolutionary genetics in infectious diseases*. **7** (3), 399-409.

Phoolcharoen W., Prehaud C., van Dolleweerd C.J., Both L, da Costa A., Lafon M., Ma J.K. (2017). Enhanced transport of plant-produced rabies single-chain antibody-RVG peptide fusion protein across an in cellulo blood-brain barrier device. *Plant biotechnology journal*. **15** (10), 1331-1339.

Power B.E., Hudson .PJ. (2000). Synthesis of high avidity antibody fragments (scFv multimers) for cancer imaging. *Journal of immunological methods*. **242** (1-2), 193-204.

Rongguang Lu Y.Y., Xiangyu Zhu, Qiumei Shi, Yang Wang, Jigui Wang, Shuang Lv, et al. (2020). Molecular characteristics of the capsid protein VP2 gene of canine parvovirus type 2 amplified from raccoon dogs in Hebei province, China. *Archives of virology*. **165** (11), 2453-2459.

Smith R.A., Zammit D.J., Damle N.K., Usansky H., Reddy S.P., Lin J.H., et al. (2021). ASN004, A 5T4-targeting scFv-Fc Antibody-Drug Conjugate with High Drug-to-Antibody Ratio, Induces Complete and Durable Tumor Regressions in Preclinical Models. *Molecular cancer therapeutics*. **20** (8), 1327-1337.

Todorova N., Rangelov M., Bogoeva V., Stoyanova V., Yordanova A., Nikolova G., et al. (2021). Anti-Idiotype scFv Localizes an Autoepitope in the Globular Domain of C1q. *International journal of molecular sciences*. **22** (15), 8288.

Tsao J., Chapman M.S., Agbandje M., Keller W., Smith K., Wu H., et al. (1991). The three-dimensional structure of canine parvovirus and its functional implications. *Science*. **251** (5000), 1456-1464.

Vives E., Brodin P., Lebleu B. (1997). A truncated HIV-1 Tat protein basic domain rapidly translocates through the plasma membrane and accumulates in the cell nucleus. *The Journal of biological chemistry*. **272** (25), 16010-16017.

Wender P.A., Rothbard J.B., Jessop T.C., Kreider E.L., Wylie B.L. (2002). Oligocarbamate molecular transporters: design, synthesis, and biological evaluation of a new class of transporters for drug delivery. *Journal of the American Chemical Society*. **124** (45), 13382-13383.

Wu B., Li M., Li K., Hong W., Lv Q., Li Y., et al. (2021). Cell penetrating peptide TAT-functionalized liposomes for efficient ophthalmic delivery of flurbiprofen: Penetration and its underlying mechanism, retention, anti-inflammation and biocompatibility. *International journal of pharmaceutics*. **598**, 120405.

Xie Y., Wang S., Yuan Q., Xie N. (2019). Advances in the research and application of cell penetrating peptides. *Chinese journal of biotechnology*. **35** (7), 1162-1173.

Xu Yongting Cy, Yu li, Tan guixiang, Tan yongjun, Huang mingmin. (2019). In vitro and in vivo Studies on the Biological Effects of Transmembrane Peptides TAT and R9. *Acta Laser Biology Sinica*. **28** (4), 323-329.

Zhang J.F., Xiong H.L., Cao J.L., Wang S.J., Guo X.R., Lin B.Y., et al. (2018). A cell-penetrating whole molecule antibody targeting intracellular HBx suppresses hepatitis B virus via TRIM21-dependent pathway. *Theranostics*. **8** (2), 549-562.